Proceedings of The National Conference
On Undergraduate Research (NCUR) 2014
University of Kentucky, Lexington
April 3-6, 2014

Convection Initiation Along the Rocky Mountain Front Range

Brian Matilla
Department of Earth and Environment
Florida International University
Miami, FL 33199

[1]Department of Atmospheric and Oceanic Sciences
University of Colorado at Boulder
Boulder, CO 80309-0311

Faculty Advisor: [1]Katja Friedrich

Abstract

Identifying the initiation and subsequent motion of thunderstorms along the Colorado Rocky Mountain Front Range continues to be a focal point in increasing forecast accuracy. Sparse knowledge of the relationship between convection initiation and orographic precipitation with low synoptic-scale forcing leads to a low degree of forecast confidence due to the strong dependency of surface atmospheric conditions. An examination of the various properties of convection initiation ties those ideas to cases where thunderstorms are generated by weak or strong synoptic forcing. A qualitative and quantitative representation of convective storm initiation patterns is made based on radar reflectivity observed between May and August of 2009 to 2012 between Denver and Fort Collins in Colorado. Locations of convection initiation are linked to topography as well as atmospheric conditions such as upper-level wind flow, surface winds, and moisture content to determine thunderstorm characteristics and potential behavior given the initial conditions. Preliminary results show that convection develops along the Front Range and then migrates to the east in times of both weak and strong synoptic forcing. Depending on the wind direction, convection initiates on the north side of the Cheyenne Ridge and Palmer Divide for northerly flow and on the east side of the Rocky Mountains for easterly flow.

Keywords: Convection Initiation; Synoptic Forcing; Rocky Mountain Front Range

1. Introduction

Convection along the Rocky Mountain areas is responsible for most summertime rainfall events observed across the Colorado Rocky Mountain Front Range (RMFR) (including cities such as Denver, Boulder, and Fort Collins). Although forecasts and measurements for summertime precipitation have increased in skill and accuracy in recent years, understanding the origin of convection initiation (CI) and subsequent development of thunderstorms lags behind. Knowledge of various temperature, wind speed and direction, and present moisture fluctuation scenarios is critical in understanding the origin of and evolution of high terrain thunderstorms and their propagation. The influence of topographic features such as mountain ranges and valleys (Palmer Divide and Cheyenne Ridge) versus certain environmental conditions can also aid in understanding how the mountain and valley breeze mechanisms play a role in the initiation phase of thunderstorms along the RMFR. Accuracy in forecasting CI episodes would improve greatly with this knowledge.

Without a significant influence of synoptic forcing mechanisms (e.g. cold front, upper-level troughs etc.), valley winds, slope winds, and mountain-plain winds tend to drive thunderstorm activity in the predominating flow. Topographic features along mountainous terrain could play a significant role in CI of organized precipitating clouds and thus greatly affect the distribution of rainfall totals in the various measuring areas.[6] Not only do thermally-

driven winds play a role in the ability to support convection, but they also aid in pushing convection either upslope or downslope from the origin. Typically, winds drive in the plain-mountain direction during the course of the day, causing a net heat gain, then reverse course during the evening leading to a net loss of heat.[11]

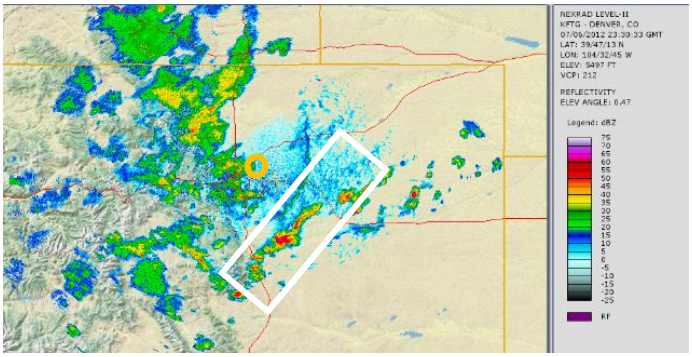

Figure 1: Radar reflectivity (color-coded) at a ~0.5º elevation angle from the Denver NEXRAD radar located in Denver, CO (orange circle) superimposed on topography and roadway network. The case shows thunderstorm development on 6 July 2012 at 2330 UTC. The area of significant convection is outlined in the white box.

Observations from operational radars along the Front Range allow for easier detection of CI. The Denver Weather Surveillance Radar, 1988, Doppler (WSR-88D) (KFTG) operated by the National Weather Service encompasses a large portion of the RMFR, thus aiding in the study of CI locations during episodes with weak and strong synoptic forcing. As an example of CI along the RMFR, Figs. 1 and 2 show the formation of convective activity in Colorado. CI can be described as the initial onset of thunderstorm activity (denoted by red colored areas, or cells). Strong updraft characteristics are due to greater evaporative cooling from precipitation, and this is commonly seen in most RMFR and high-plains convection. Because air from the resulting downdraft is cooler than its surroundings, this creates outflow boundaries usually denoted on radars as a vague radar reflectivity that races ahead of the parent cell. These outflow boundaries usually are observed to have reflectivities below 30 decibels of Z, or dBZ (see Fig. 1). In some cases, outflow boundaries act as a secondary forcing mechanism in RMFR CI, and will usually intensify or generate new convective activity ahead of the parent cell.[14]

Many studies have been performed over the past few decades regarding RMFR CI and the roles of certain mesoscale patterns allowing for intensification of such storms.[1,12,10,15] The RMFR with the north-south oriented Rocky Mountains to the west is considered a conducive environment for CI, especially during the summer season where the possibilities of severe convective systems can emerge due to daytime heating and upper-level favorability.[12] Smaller topographic features including the west-east oriented Palmer Divide to the south and the west-east oriented Cheyenne Ridge to the north are responsible for developing the Denver Convergence Vorticity Zone (DCVZ). Shown in Fig. 2, moist air moves into the region from the southeast and interacts with the Palmer Divide and the northwest wind flow from the north-south axis of the RMFR. The result is a cyclonic flow near the surface and subsequent thunderstorm development over the Denver metropolitan area.[9,8] The DCVZ can play a significant role in the development of orographic precipitation and CI episodes over the RMFR and surrounding region.

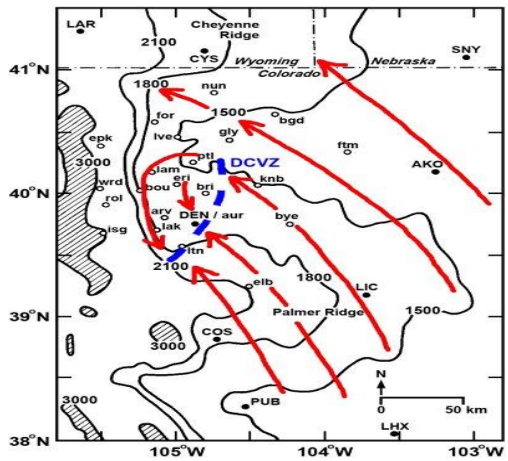

Figure 2: Schematic of the Denver Convergence Vorticity Zone showing the typical wind flow structure along the RMFR.[2]

Typically, convection occurs with the advent of daytime heating and upper-level instability. In this study, a determination of CI locations within the range of KFTG during days with weak and strong synoptic forcing was made in order to understand if there is a significant correlation between CI locations, topography, and general wind direction. Also, CI locations during weak and strong synoptic forcing were studied to determine if there are patterns in CI locations.

2. Data and Methods

2.1 Case Selection

The KFTG radar data and radar composite maps from the University Corporation for Atmospheric Research's archive were used to monitor thunderstorm development (shown in Fig. 1) and determine days with thunderstorm development over the RMFR between May and August of 2009 to 2012. The cases were determined to be CI events if isolated thunderstorm cells of enhanced reflectivity (greater than 35 dBZ) were observed within the viewing area of KFTG (~230 km) (see Fig. 1). Thunderstorm development may occur as a result of either weak or strong synoptic forcing. Once an episode of CI was identified, archived surface and 500 hectopascal (hPa) maps from the National Oceanic and Atmospheric Administration's (NOAA) Weather Prediction Center were used to determine whether the event had weak or strong synoptic forcing. To classify an episode with weak synoptic forcing, there must be the lack of any surface frontal systems and a presence of an upper-level ridge at 500 hPa (example in Fig. 3.). For episodes with strong synoptic forcing, there would need to be a surface frontal system or associated low pressure system moving through Colorado that is confirmed by the presence of an upper-level trough (seen in Fig. 4.).

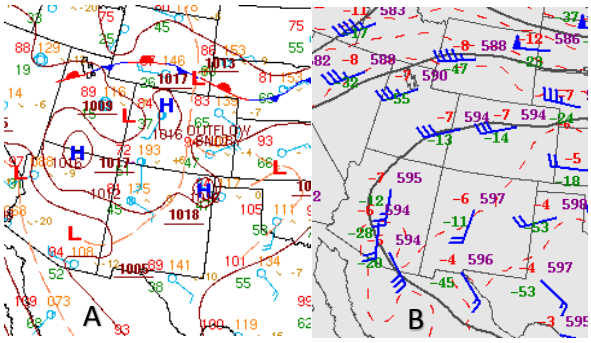

Figure 3: Surface conditions chart (A) and upper atmospheric conditions chart (B) to 500 hPa (~18,000 feet) from 11 July 2009. Conditions are indicative of weak synoptic forcing.

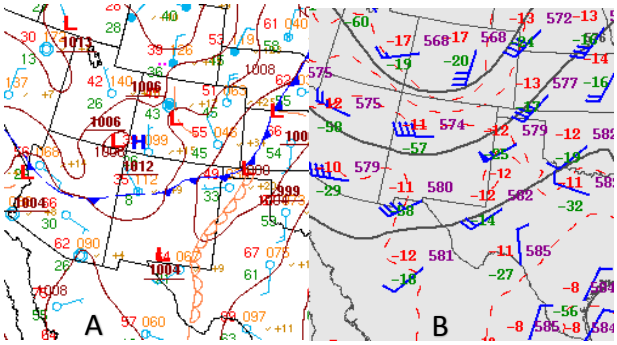

Figure 4: Same as figure 3; from 19 May 2012. Conditions are indicative of strong synoptic forcing.

2.1.1 radar data

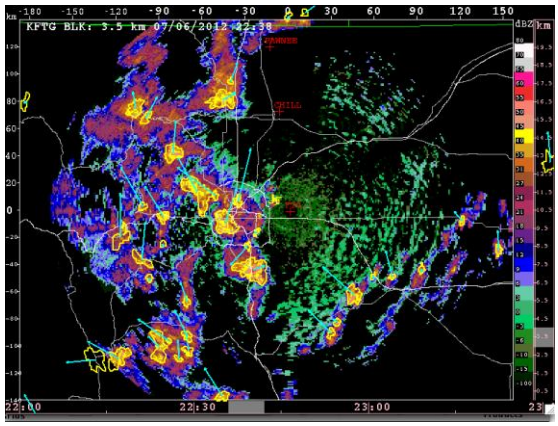

Figure 5: CIDD interface displaying radar reflectivity (color-coded) and results from the cell tracking algorithm TITAN on 6 July 2012 at 2238 UTC. The yellow outlines indicate individual thunderstorm cells and blue arrows indicate TITAN's prediction of the storms' motion.

The radar reflectivity from KFTG's Level II radar data was used to determine CI location. For days with active convection over the RMFR, data was downloaded from NOAA's National Climatic Data Center archive (http://www.ncdc.noaa.gov/nexradinv/). Note that the maximum range of KFTG is limited to about 230 km. Since the dual-polarization radar upgrades were completed on the WSR-88D radars nationwide, reflectivity is denoted as Z_H due to the introduction of horizontal polarization being transmitted and received simultaneously and subsequent calibration of such horizontal variables.[3] Due to the radar scan strategy, near-surface features (e.g., gust fronts) within the ~700 m AGL were visible up to roughly 80 km at the lowest elevation angle of 1 degree. It is worth noting that these are just general guidelines since vertical refractivity gradients play a key role in distinguishing enhanced reflectivity cells and there such lies a potential uncertainty. Also, elevation angles ranging from 0.95 to 19.5 degrees provide sufficient information about thunderstorm structure.[7]

To explore the nature of each individual cell, the Thunderstorm Identification, Tracking, Analysis, and Nowcasting (TITAN) algorithm was used to track individual thunderstorm cells. The Cartesian Interactive Data Display (CIDD) was used to visualize the radar reflectivity and results from the TITAN algorithm. Once the thunderstorm reaches a set reflectivity threshold ($Z_H > 35$ dBZ), TITAN automatically creates a polygon to the shape of the thunderstorm cell while also determining the potential path at the next scan time, viewable in CIDD (Fig. 5). TITAN also creates a data output providing the location of CI for each individual convective cell in a given CI episode, and the output plots can be seen in Figs. 7a and 8a.

2.1.2 sounding and tower observations

The National Wind Technology Center (NWTC) is located about 65 km northwest of Denver. It is located close to the Front Range, i.e., the area of CI. Wind velocity and wind speed observations were obtained from NWTC's Baseline Measurement System tower at 42 m AGL using the Met One Instruments WS-201 wind sensor system in order to determine near-surface wind behavior. The measurements were accumulated each minute and had an accuracy of ±3.6° for wind direction and ±0.5 ms^{-1} for wind speed.[4] Data was obtained from the NWTC archives for the duration of the CI episode. For this experiment, observations from the NWTC were the sole resource analyzed, so it is important to note the potential for low-level wind estimate uncertainties.

In addition, operational upper-air soundings launched at 0000 and 1200 UTC from Denver International Airport were utilized in order to determine atmospheric stability. The relationship between air temperature and dew point can detail information about atmospheric moisture concentration. In essence, a smaller difference between the air temperature and dew point indicates a moist atmosphere while a larger difference would signal a drier environment. These two profiles will allow for a better understanding of environmental conditions where CI would take place. An example of wind and stability information obtained during an event, discussed in more detail in section 3, is given in Fig. 6.

A

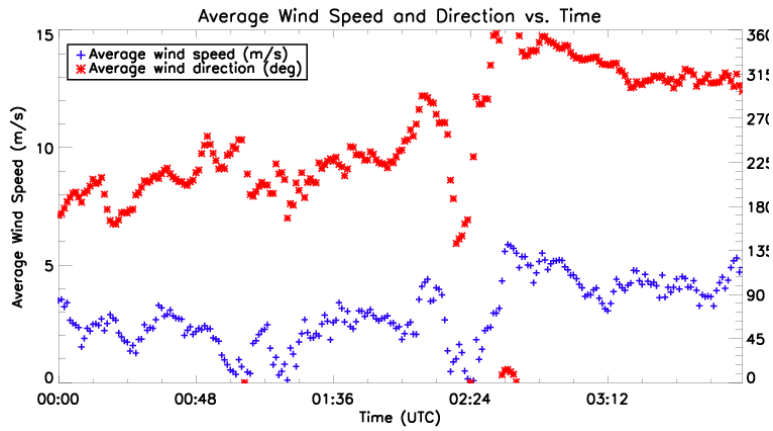

B

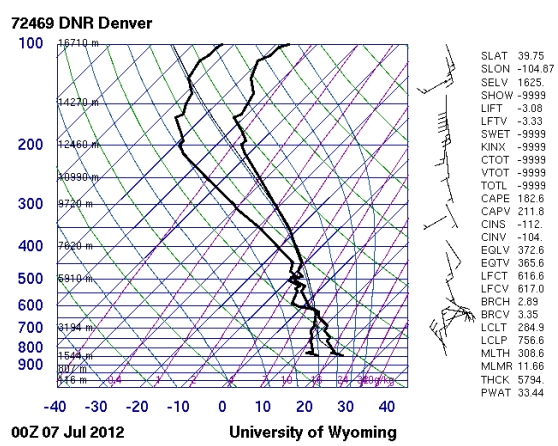

Figure 6: A plot of near-surface wind speed and direction versus time during a CI episode on 11 July 2009 (A), and a Denver, CO upper air sounding from 7 July 2012, both at 0000 UTC (B). The sounding shows variable wind barbs with increasing height in the atmosphere, as well as the change of dew point (left) and air temperature (right) with increasing height.[11]

3. Preliminary Results

Table 1: Identified CI cases (no particular order) and their respective synoptic forcing classification and approximated CI start time. Cases analyzed are bolded.

Date	*Classification*	*Approx. CI start (UTC)*			
7 June 2012	Weak	2000	30 May 2010	Strong	0100
23 June 2009	Weak	2100	**19 May 2012**	**Strong**	**1100**
1 June 2009	Weak	2000	8 June 2011	Strong	1900
9 July 2009	Weak	2100	9 June 2011	Strong	2000
11 July 2009	**Weak**	**0000**	**22 Aug 2012**	**Strong**	**2000**
29 July 2009	**Weak**	**2000**	31 Aug 2009	Strong	1900
9 July 2010	Weak	1900	18 Aug 2012	Strong	0900
21 July 2010	Weak	2000			
13 July 2011	Weak	2000			
7 July 2012	**Weak**	**2000**			
31 July 2012	**Weak**	**2000**			
22 July 2010	Weak	2000			
2 July 2012	**Weak**	**2200**			
22 July 2012	Weak	2000			
4 July 2010	Weak	2100			
4 Aug 2011	Weak	2200			
25 Aug 2009	Weak	1900			
9 Aug 2010	Weak	0200			
28 Aug 2011	Weak	2000			
10 Aug 2009	Weak	0500			

Table 1 contains the total amounts of CI cases identified for each month for the period 2009 through 2012 including specific details regarding CI start times and dates (UTC to MDT is -6 hours). These cases were observed to exhibit a noticeable CI event across the RMFR around the late evening or early morning hours without any previously established convection. Most cases would usually occur for a period between 4-6 hours from the initial start time (not shown). July was found to have a larger amount of overall cases compared to the other months, largely due in part to the onset of the North American Summer Monsoon.[5] Of the 27 identified cases , four are shown in Figs. 7-8 consisting of two cases with weak synoptic forcing and two with strong synoptic forcing.

3.1 Cases Of Convection Initiation During Weak Synoptic Forcing

Fig. 7 shows the location of CI as a function of time during two periods of weak synoptic forcing, as well as near-surface wind speed and direction plots for each episode. In these two episodes, it was observed that most of the early convection initiated over the Rocky Mountains (within the first 2 hours after the initial convection start time). Later convection would be generated along a greater area of the Palmer Divide, with several cells generating along the Cheyenne Ridge for the episode on 31 July 2012. For near-surface winds, a general southerly wind flow was found during the early stages of CI on both days, shifting to a northerly flow near the end of the episode (Fig. 7b). The wind shift is most likely a result of small-scale feedback mechanisms related to changes in the diurnal heating cycle between the plains and the mountains due to convective activity itself changing atmospheric stability due to latent heat exchange. Despite that, even with a light wind speed of about 5 ms^{-1} at the surface, the general pattern for CI movement is guided by the uniform westward to southwestward upper-level wind component indicative of zonal flow being present over the RMFR as shown in the upsonde data. A generally dry atmosphere was observed with few areas of increased moisture in the upper-levels but it is worth noting that the cyclonic wind flow near the surface

is representative of the typical DCVZ wind pattern. Convective cells were still generated in these episodes despite a generally stable environment.

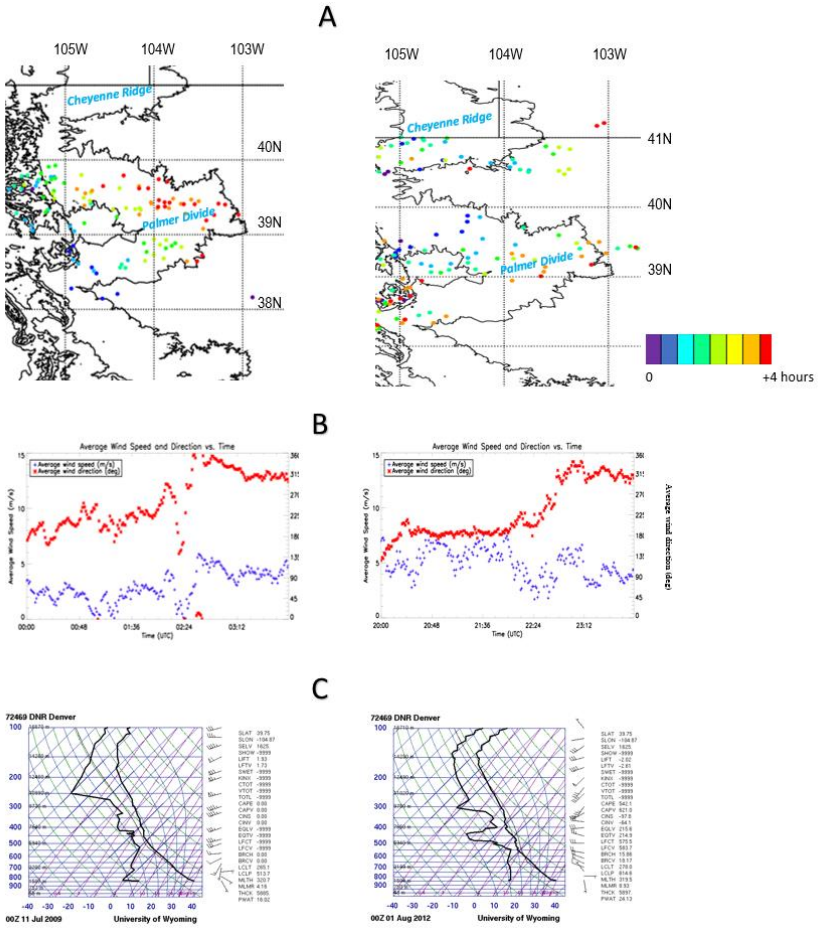

Figure 7: CI location, surface wind plot, and upper air sounding mosaic for 11 July 2009 from 0000-0400 UTC (left column) and 31 July 2012 2000-0000 UTC (right column). Earlier convection indicated by purple and blue dots; later convection (up to 4 hours later) indicated by oranges and reds. Each new color represents a 30 minute interval (A). Lower images describe wind characteristics during the CI episodes where red marks indicate wind direction and blue marks show wind speed (B). Upper air sounding information is described in figure 6 (C).

3.2 Cases Of Convection Initiation During Strong Synoptic Forcing

In Fig. 8, both cases shown depict convection initiating primarily along the boundary propagating eastward as the frontal boundary progresses. Note that radar coverage of KFTG is limited to the east of the Continental Divide. As such, it is found that convection initiates near the Rocky Mountains propagating eastward with time. Near surface winds showed a westward component at the surface and upper-levels for a majority of the time during the episodes. There was also a greater correlation in organized CI with a uniform westward wind direction as opposed to a gradual shift in direction with height (22 August and 19 May, respectively). Higher moisture content was found in these cases, especially during the 19 May 2012 episode (see Fig. 8c left). Higher moisture content, cooling at the upper-levels, and presence of a certain weather system over the RMFR all combined to increase instability during these episodes. Coupled with the DCVZ wind pattern and topographic features of the RMFR, this atmospheric destabilization can allow for convective cells to develop with less environmental resistance.

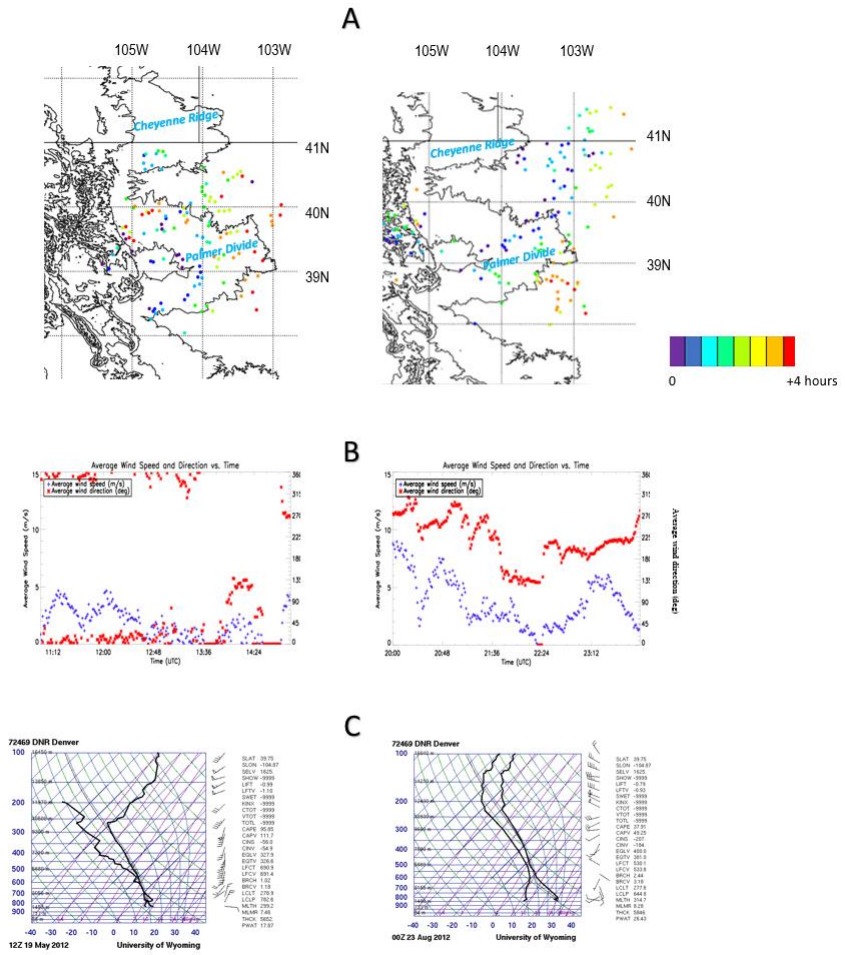

Figure 8: Same as figure 7; 19 May 2012 1100-1500 UTC (left column) and 22 August 2012 2000-0000 UTC (right column).

4. Discussion

There is still plenty of work to be done in order to draw a substantial conclusion. However, based on the evidence obtained, it was found that CI follows a similar pattern in both weak and strong synoptic forcing. In the weak synoptic forcing conditions, primary CI takes place over the RMFR, Palmer Divide and Cheyenne Ridge depending on the wind direction. The CI is most likely linked to regional wind pattern associated with differences in the radiative budget between the mountains and the plains. With passing time, most of the newer CI would take place over the Palmer Divide, portions of the Cheyenne Ridge, and into the Great Plains most likely associated with outflow boundaries from older thunderstorms. The surface wind charts showed that there is a consistent change in wind direction, primarily from southwest to north or northwest. In the two strong synoptic forcing conditions presented here, convection initiated along the surface boundary, first close to the mountains and later farther to the east as the cold front propagated eastwards. It is also worth noting that, concurrent with the DCVZ information mentioned earlier, most CI is enhanced by the topographic features of the Palmer Divide and Cheyenne Ridge due to the general area of CI activity in most cases as shown by the sounding data. The influence of the RMFR can provide much of the northwest steering flow seen at the upper-levels of the atmosphere. In the process, valley winds from the southeast can interact with these northwest winds which can cause uplift over the Palmer Divide, helping to generate CI. This is represented by the cyclonic wind flow near the surface in most of the soundings during a CI episode.

A majority of cases of CI with weak synoptic forcing began around 2000 UTC (~2:00 PM Mountain Daylight Time), but all cases lasted for a period of 4 to 6 hours. In those cases, it is primarily due to the daily heating of the surface from sunlight. The air mass over the mountains can reach the convective temperature more easily during the summer months compared to the air mass over the Great Plains.[8] Warmer air at the surface with colder air aloft destabilizes the atmosphere and, when coupled with the typical steering flow in the upper-levels, the result is CI over the RMFR region with propagation to the east during the afternoon and evening.

5. Future Plans

Future studies in CI involve a continuation of the analysis with the remaining cases. The inclusion of wind data from the Automated Surface Observing System is expected to provide a better understanding of surface and upper level wind behavior. There will also be in-situ observations along the RMFR. An analysis of atmospheric temperature and humidity profiles will be included along with further studies on upper-level and surface wind profiles. Also, moisture flux and Froude values for each case of weak and strong synoptic forcing will be taken since this is necessary to better understand the behavior of wind and moisture in the atmosphere as it passes over the RMFR and into the Great Plains. In addition, further analysis of both weak and strong synoptic forcing cases will be done in order to study the cloud microphysical structures in the individual thunderstorms. This also will involve the analysis of primary and secondary CI within individual episodes. Rainfall characteristics, vertically integrated liquid, and echo tops are some of the parameters to be studied in understanding the evolution of RMFR thunderstorms into potentially severe thunderstorms over the Great Plains. Finally, the introduction of the dual-polarization upgrade for the weather surveillance radars can provide extra information in understanding certain microphysical processes during CI events.

6. Acknowledgements

Much of the resources used to compile and analyze the data were provided by the Department of Atmospheric and Oceanic Sciences at the University of Colorado in Boulder, CO, as well as the National Center for Atmospheric Research. The wind tower data for surface observations was provided by the National Renewable Energy Lab. The University of Wyoming Department of Atmospheric Sciences provided the upper air sounding data. Funding and guidance for conducting this research was provided by the University of Colorado-Boulder Summer Multicultural Access to Research Training program and by the Ronald E. McNair Post Baccalaureate Achievement Program of Florida International University.

7. References

1. Burghardt, B. (2013). *Assessing The Predictability of Convection Initiation Using an Object-Based Approach.* Milwaukee: The University of Wisconsin- Milwaukee. Retrieved from http://dc.uwm.edu/cgi/viewcontent.cgi?article=1085&context=etd
2. Egger, C. (n.d.). *Colorado's Front Range: Understanding Tornadogenesis in relation to the Denver Cyclone.* Retrieved from The Weather Prediction: http://www.theweatherprediction.com/weatherpapers/013/
3. Gourley, J., Illingworth, A. J., & Tabary, P., 2009: Absolute calibration of radar reflectivity using redundancy of the polarization observations and implied constraints on drop shapes. J. Atmos. Oceanic Technol., 26, 689–703. doi: http://dx.doi.org/10.1175/2008JTECHA1152.1
4. Friedrich, K., Lundquist, J. K., Aitken, M., Kalina, E. A., & Marshall, R. F., 2012: Stability and turbulence in the atmospheric boundary layer: A comparison of remote sensing and tower observations. Geophys. Res. Lett., Vol. 39, No. 3, L03801, doi:10.1029/2011GL050413.
5. Grantz, K., Rajagopalan, B., Clark, M., & Zagona, E. (2007). Seasonal Shifts in the North American Monsoon. *Journal of Climate, 20*(9), 1923-1935. doi:10.1175/JCLI4091.1
6. Houze , R. A. (2012, January 6). Orographic effects on precipitating clouds. *Reviews of Geophysics, 50*(1), 47. doi:10.1029/2011RG000365

7. Huber, M., & Trapp, J. (2009). A Review of NEXRAD Level II: Data, Distribution, and Applications. *Journal of Terrestrial Observation, 1*(2), 5-16. Retrieved July 31, 2013, from http://docs.lib.purdue.edu/cgi/viewcontent.cgi?article=1042&context=jto
8. Meyer, T. A., Bobb, W. R., & Dulong, T. W. (1999). Denver Air Route Traffic Control Thunderstorm Patterns. *Denver Air Route Traffic Control Thunderstorm Patterns*, 15. Longmont, Colorado, United States of America. Retrieved August 5, 2013, from http://www.crh.noaa.gov/zdv/zdvtstms.pdf
9. Pietrycha, A. E., & Rasmussen, E. N. (2001). *Observations of the DCVZ using mobile Mesonet data.* Ninth Conference on Mesoscale Processes. Fort Lauderdale: American Meteorological Society. Retrieved from https://ams.confex.com/ams/pdfpapers/22299.pdf
10. Schaaf, C. B., Wurman, J., & Banta, R. M. (1988, March). Thunderstorm-Producing Terrain Features. *Bulletin of the American Meteorological Society, 69*(3), 272-277. doi:10.1175/1520-0477(1988)069<0272:TPTF>2.0.CO;2
11. Serafin, S., & Zardi, D. (2010, November). Daytime Heat Transfer Processes Related to Slope Flows and Turbulent Convection in an Idealized Mountain Valley. *Journal of the Atmospheric Sciences, 67*(11), 3739-3757. doi:10.1175/2010JAS3428.1
12. Tucker, D. F., & Crook, A. N. (1999, June). The Generation of a Mesoscale Convective System from Mountain Convection. *Monthly Weather Review, 127*(6), 1259-1273. doi:10.1175/1520-0493(1999)127<1259:TGOAMC>2.0.CO;2
13. University of Wyoming. (2012, July 7). *Department of Atmospheric Sciences*. Retrieved July 13, 2013, from http://weather.uwyo.edu/upperair/sounding.html
14. Wilson, J., & Schrieber, W. (1986, December). Initiation of Convective Storms at Radar-Observed Boundary Layer Convergence Lines. *Monthly Weather Review, 114(*12*),* 2516-2536. doi:10.1175/1520-0493(1986)114<2516:IOCSAR>2.0.CO;2
15. Zardi, D., & Whiteman, D. C. (2012). Diurnal Mountain Wind Systems. In *Mountain Weather Research and Forecasting* (pp. 35-119). Salt Lake City: Springer Netherlands. doi:10.1007/978-94-007-4098-3_2